

Application of chitosan/Al₂O₃ nano composite for the adsorption of thorium (IV) ion from aqueous solution

B. Rouhi Broujeni^a, A. Nilchi^b, A.H. Hassani^{a,*}, R. Saberi^b

^aDepartment of Environment and Energy, Tehran Science and Research branch, Islamic Azad University, Tehran, Iran, email: babak.rouhi@srbiau.ac.ir (B.R. Broujen), ahh1346@gmail.com (A.H. Hassani)

^bMaterials and Nuclear Fuel Research School, Nuclear Science and Technology Research Institute, P.O. Box 11365/8486, Tehran, Iran, email: anilchi@aeoi.org.ir (A. Nilchi), rsaberi@aeoi.org.ir (R. Saberi)

Received 16 July 2017; Accepted 5 December 2017

ABSTRACT

In this study, novel chitosan/Al₂O₃ nano composite (Ch/Al-O_{NC_o}) was synthesized and evaluated as an adsorbent for removing thorium (IV) (Th⁴⁺) ion from aqueous solution. The Ch/Al-O_{NC_o} was characterized by X-ray diffraction (XRD), Brunauer–Emmett–Teller (BET), Fourier Transform Infrared (FT-IR) and Scanning Electron Microscopy (SEM) and the specific surface area of Ch/Al-O_{NC_o} were found to be 29.23 m²g⁻¹. Batch experiments were carried out under varying operating conditions namely adsorbent weight, contact time and initial pH. The optimum adsorbent weight was found to be 0.2 g L⁻¹ while the adsorption process was found to be optimal in the wide pH range of 2–8. The adsorption kinetics was well described by the pseudo-second-order equation, when the Langmuir model better fit the adsorption isotherms. The adsorption capacity of Ch/Al-O_{NC_o} was 591.12 mg Th⁴⁺/g composite, leads to 99% removal at 25°C. Moreover, the calculated thermodynamic parameters including standard enthalpy, entropy, and Gibbs free energy indicates the spontaneous and endothermic nature of the adsorption process. The loaded Th⁴⁺ can be easily regenerated with HNO₃ and the Ch/Al-O_{NC_o} could be used repeatedly without any significant reduction in its adsorption capacity. The desorption level of Th⁴⁺ from the Ch/Al-O_{NC_o} by using 0.1 M HNO₃ was more than 94%.

Keywords: Nano aluminum oxide; Chitosan nanocomposite; Hydrothermal; Adsorption; Th⁴⁺

1. Introduction

Industry development in the whole world has led to increase in production of industrial waste and consequently the entry of toxic and hazardous ions such as radioactive ions to the environment [1]. These ions have high toxicity even in very low concentrations and are extremely harmful for the environment and health [2]. One of the major radioactive ions that is very useful as a nuclear fuel and is found in wastewaters resulting from the production of nuclear fuels is Th⁴⁺, which can be used as nuclear fuel by conversion into uranium-233 (²³³U) [3,4]. Soil, rocks, sand and water are the main source of thorium and because its availability is 3 to 4 times higher than uranium, this ion has

attracted a lot of interest as a nuclear fuel [5,6]. In addition, in the cycle of using thorium as the primary fuel, the raw material is less used and consequently, the waste produced is less too [7]. Moreover, other thorium compounds and alloys have various applications; for example, thorium is used in high-quality lenses or the manufacture of ceramics at high temperatures [8]. Therefore, considering the extensive use of thorium in industries and its long-term stability in the environment, as well as its potential damage to human health and the environment, the removal and recovery of this ion from wastewaters is essential [9].

Several methods have been used for the recovery of thorium from waste containing this ion. Some of these methods are solvent extraction, chemical precipitation, ion exchange, evaporation, biosorption and adsorption

*Corresponding author.

[10–16]. Many of these methods can be criticized from different points of view such as the economic, health and production of hazardous wastes [17]. Among the described techniques, adsorption is one of the most common methods of removing heavy metals from aqueous solutions, due to its features such as high efficiency, low cost, easy reduction and lack of sludge production [18].

One of the abundant polymer adsorbent in nature is chitosan (Ch). Ch is a biopolymer, which can be achieved from chitin by deacetylation [19]. Ch has the highest capacity and great potential to adsorb metal ions compared to other biopolymers, due to attendance of active functional groups such as hydroxyl and amino in its structure [20,21]. However, Ch has some weak points such as softness, tendency to agglomerate or form gels, low porosity, low surface area, hydrodynamic limitations in adsorption column and non-availability of reactive binding sites [22,23]. In this context, recent research has inclined to modify and combine Ch with other adsorbents [24–26]. There are a number of researches on the adsorption of radioactive ions by Ch and its derivatives [2,20,27,28], but only few papers are available on the usage of Ch-based nanocomposites. For example, ethylenediamine-modified magnetic Ch particles were reported to adsorb radioactive uranyl ions [29]. In similar studies, the adsorption of thorium and uranyl ions by unmodified magnetic Ch particles have reported [30].

This study presents the preparative conditions, adsorption properties and analytical applications of novel Ch/Al-O_{NC_o} as an adsorbent for the removal of Th⁴⁺ from aqueous solution. The synthesized Ch/Al-O_{NC_o} was characterized and its adsorption properties for the removal of Th⁴⁺ under varied experimental conditions were investigated. The adsorptive features were appraised based on adsorption parameters obtained from the compatibility of adsorption isotherms to the Langmuir and Freundlich models. In addition, kinetic data have modeled by the pseudo-first and second-order kinetic models. All the experiments and analyses were carried out in laboratories of nuclear science and technology research institute of Iran.

2. Experimental

2.1. Material and method

All the selected reagents were of analytical grade and purchased from Merck. The stock solutions for preparation of Th⁴⁺ were prepared by dissolving thorium salt (Th(NO₃)₄·5H₂O) in deionized water. The initial pH of solutions was adjusted by nitric acid (HNO₃; 99.9%) or sodium hydroxide (NaOH; 99.9%) solutions and Metrohm pH meter model 744. Sartorius Electrical Balance Model BP 221S, Laboren oven, Nabertherm furnace, thermostated shaker and mixer HT Infors AG model CH-4103-BOT Tmingen were used to conduct the experiments. The synthesis of adsorbent was carried out by using hydrothermal reactor which was designed and made of stainless steel 316L as well as conventional autoclaves with Teflon liner by volume of 100 mL. All the experimental data were the averages of duplicate experiment, and the average relative error is less than 5%.

2.2. Synthesis of Al₂O₃ nano particle (Al-ONPs)

Al-ONPs was prepared by hydrothermal synthesis method. 18.75 g Al(NO₃)₃ and 6 g CH₄N₂O was dissolved in 125 mL of distilled water at temperature 70°C and stirred for 2 h. The solution was poured into hydrothermal reactor and put in hydrothermal autoclave at 200°C for 24 h. The produced Al-ONPs was washed with deionized water and dried at room temperature. A mixture of water and ethanol (1:5 (v/v)) was added drop wise to the suspensions of Al-ONPs under vigorous magnetic stirring and left to stir for 1 h. The modified Al-ONPs was washed with ethanol for several times and dried in the oven, at 120°C for 2 h.

2.3. Synthesis of Ch/Al-O_{NC_o}

Ch medium molecular weight with the degree of deacetylation between 75–85% was used in order to prepare Ch/Al-O_{NC_o}. 1.67 g Ch was dissolved in 50 ml of 0.1 M HCl solution and stirred for 1 h. Then 0.1 g of the prepared Al-ONPs in 10 mL/L HCl solution was fully dispersed in the Ch acidic solution. A sampler was used to drip out the resulting solution into 0.1 M NaOH solutions. Droplets formed as spherical nanocomposites with a diameter of 0.4 cm. The resulting Ch/Al-O_{NC_o} were maintained in NaOH solution for 24 h and finally, washed with deionized water and dried at room temperature. The preparation procedure and the produced Ch/Al-O_{NC_o} are presented in Figs. 1 and 2.

2.4. Adsorbent characterization

Phase identification, crystallite size and the composition of the products were characterized by XRD obtained on Philips Xpert diffractometer using a scan rate of 2°/min and CuKα line (λ = 1.54056 Å) radiation with working voltage and current of 40 kV and 40 mA, respectively. SEM (Cambridge S-360) studied the morphology of the product.

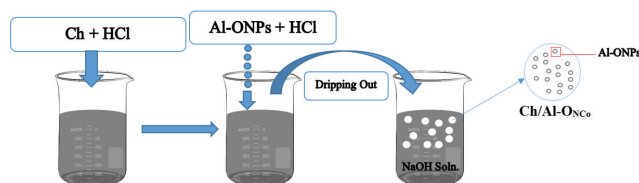


Fig. 1. Ch/Al-O_{NC_o} preparation procedure schematic.



Fig. 2. Sample of Ch/Al-O_{NC_o} synthesized in the laboratory.

BET specific surface area was determined through nitrogen adsorption isotherms using Quantachrome NOVA 2200e system. Qualitative chemical structure assessment was carried out by FTIR analysis (Vector22 Bruker Company, USA). Th⁴⁺ analysis was carried out using a Perkin-Elmer Optima 2000 DV model Inductively Coupled Plasma-Optic Emission Spectrometry (ICP-OES).

2.5. Sorption experiments

Batch experiments were conducted to study the extent of Th⁴⁺ adsorption by Ch/Al-O_{NC_o} in a polyethylene tube. The solution containing 0.02 g Th⁴⁺ ions was mixed with the adsorbent at different weight (0.05–0.25 g), contact time (20–80 min) and pH values (2.0–8.0). In a typical experiment, a desired amount of adsorbent was added to a tube containing 100 mL solution of Th⁴⁺ (200 mg L⁻¹). Then the tube was placed in a thermostated shaker at 150 rpm. The initial pH of the Th⁴⁺ solutions was adjusted by adding 0.01 M HNO₃ or NaOH solutions. Following the adsorption procedure, the Ch/Al-O_{NC_o} was separated by filtration and the residual concentration of the Th⁴⁺ ion was determined. In order to explore thermodynamic parameters, experiments were carried out at the optimized value of variables at five different temperatures (25, 30, 35, 40 and 45°C). The adsorption percentage (Ads %) and the amount of metal ion sorbed at time t (q_e and q_t , mg g⁻¹) were calculated using Eqs. (1) and (2):

$$Ads\% = \frac{C_0 - C_e}{C_0} \times 100 \quad (1)$$

$$q_e = \frac{C_0 - C_e}{m} \times V; \quad q_t = \frac{C_0 - C_t}{m} \times V \quad (2)$$

where C_0 is the initial metal ion concentration (mg L⁻¹), C_e is the amount of metal present in the solution at equilibrium (mg L⁻¹), V is the volume of thorium solution (L) and ' m ' is the dry weight of sample (g).

The adsorption process, described by the ion distribution coefficient, K_d (mL g⁻¹), was calculated using Eq. (3):

$$K_d = \frac{C_0 - C_e}{C_e} \times \frac{V}{m} \quad (3)$$

2.6. Desorption experiments

Desorption experiments were carried out in batch system using 0.1 M aqueous solutions of different reagents such as NaOH, NaCl, HCl and HNO₃. The Ch/Al-O_{NC_o} was put in contact with the desorption solution for 24 h. The amount of Th⁴⁺ ion released into solution was measured by the ICP spectrophotometric method. The Th⁴⁺ recovery percentage upon desorption from the Ch/Al-O_{NC_o} was calculated using Eq. (4):

$$Desorbed(\%) = \left(1 - \frac{Th_{ads}^{4+} - Th_{des}^{4+}}{Th_{ads}^{4+}} \right) \times 100 \quad (4)$$

where Th_{ads}^{4+} is the amount of adsorbed Th⁴⁺ (mg g⁻¹) and Th_{des}^{4+} is the amount of desorbed Th⁴⁺ (mg g⁻¹).

The reusability was investigated by repeating the adsorption–desorption round up for three times and

thereby checked out the long-term adsorption potential of Ch/Al-O_{NC_o}.

3. Results and discussion

3.1. Characterization of Ch/Al-O_{NC_o}

Fig. 3 depicts XRD patterns of Ch, Al-ONPs and Ch/Al-O_{NC_o}. The XRD pattern of Ch represents broad diffraction peaks at $2\theta = 9.5^\circ$ and 19.5° which are common fingerprints of crystal Ch [31]. It was also observed that the 2θ values at the peak points of Ch/Al-O_{NC_o} are the same as those in Al-ONPs. Thus, their crystalline structure is very similar. Furthermore, comparing the XRD patterns indicates that Al-ONPs have been loaded on Ch.

The structure of Ch/Al-O_{NC_o}, Ch and Al-ONPs was confirmed by FTIR analysis (Fig. 4). The spectra of Ch showed a broad adsorbance at 3405–2985 cm⁻¹ (combined peaks of the NH₂, hydroxyls and OH group stretching vibration), at 2921 cm⁻¹ and 2360 cm⁻¹ (CH₃ and CH₂ in Ch structure), at 1635–1022 cm⁻¹ (attributed to the CONH₂ group), at 848 cm⁻¹ and 594 cm⁻¹ (CH bending of amide bonds stretching vibrations) in Figs. 4A and B. In the Fig. 4B, the peaks at 505 cm⁻¹ and 455 cm⁻¹ related to Al-O group of Al-ONPs.

The nitrogen adsorption and desorption studies showed the BET surface area of Ch/Al-O_{NC_o} site was 29.23 m²/g.

The surface structural features of Al-ONPs and Ch/Al-O_{NC_o} were studied using SEM (Fig. 5). As it can be seen in Fig. 5, Al-ONPs are in spherical shape with diameter less than 100 nm. In addition, the final products display aggregation because of Al-ONPs fixing and trapping inside the Ch. Furthermore, it was found that there were many pores

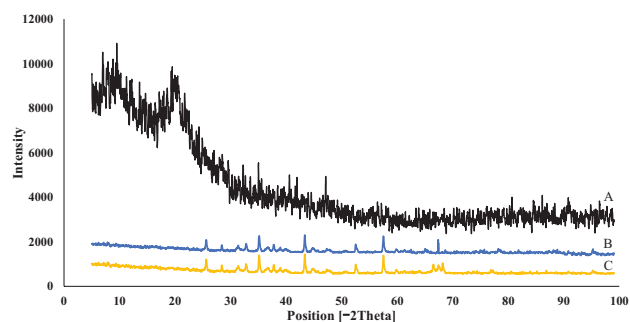


Fig. 3. XRD patterns of Ch (A), Al-ONPs (B) and Ch/Al-O_{NC_o} (C).

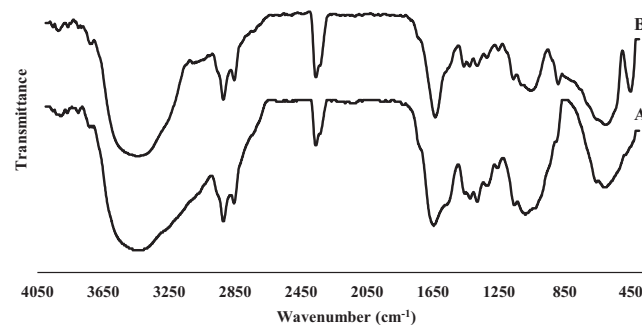


Fig. 4. FTIR spectra Ch (A), and Ch/Al-O_{NC_o} (B).

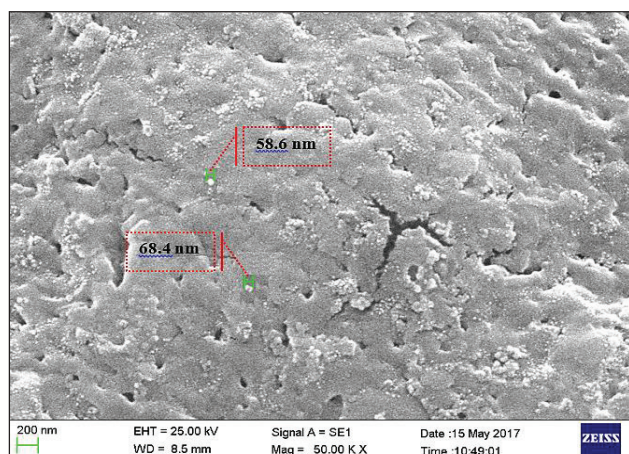


Fig. 5. SEM micrographs of Ch/Al-O_{NCo}.

and pleats on the surface of the composites, which provided active sites for Th⁴⁺ capture. The SEM picture of Ch/Al-O_{NCo} also reveals that there is a linear crack on the surface, which verifies the miscibility of the prepared polymer composite. Similar morphology features were reported for poly (methacrylic acid)-grafted Ch/bentonite composite by Anirudhan et al [20].

3.2. Effect of adsorbent weight

The effect of the adsorbent weight used on Th⁴⁺ adsorption was studied within the range of 0.05–0.25 g of adsorbent (Fig. 6). It was observed that both Ads% and the K_d continuously increase with increasing the adsorbent weight. The maximum value of Ads% and K_d obtained were 54% and 2.97, respectively. Increment in adsorption capacity with increase in adsorbent weight was expected due to the availability of a higher number of adsorbing active sites [32].

3.3. Effect of contact time

The effect of contact time on adsorption of Th⁴⁺ onto Ch/Al-O_{NCo} was studied within the range of 20–80 min (Fig. 7). According to the Fig. 7, by increasing the contact time, the Th⁴⁺ ion adsorption increased rapidly within 50 min due to the plentiful availability of reaction sites and slowly at about 60 min. Optimum contact time was found to be 70 min, which resulted in 91% adsorption. The achievement of equilibrium adsorption might have been due to the reduction in the available active adsorption sites on the adsorbent with time resulting in limited mass transfer of the adsorbate molecules from the bulk liquid to the outer surface of adsorbent.

3.4. Effect of pH

pH changes are effective in adsorbent's capability in very complex adsorption processes. Accordingly, experiments were conducted in order to examine the effect of pH on Th⁴⁺ removal by changing the pH from 2.0 to 8.0. (Fig. 8). Based on Fig. 8, pH was a controlling factor in Th⁴⁺ adsorption. As pH increased from 2.0 to 4.0, the fraction of Th⁴⁺

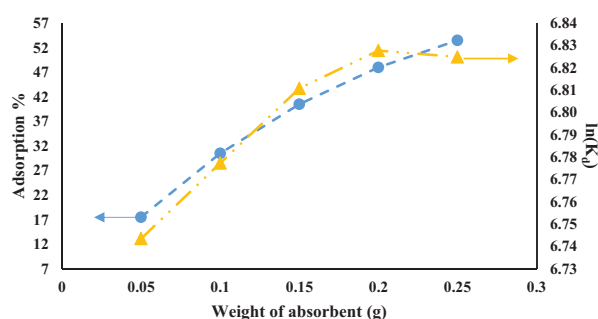


Fig. 6. Effect of adsorbent weight on Th⁴⁺ adsorption and distribution coefficient. Contact time 10 min, pH of 7, 200 mg L⁻¹ Th⁴⁺ and at 25°C temperature.

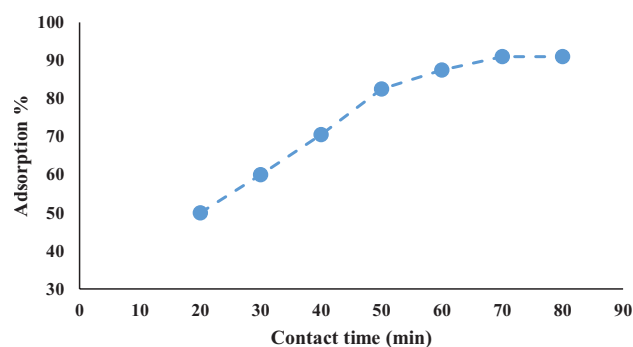


Fig. 7. Effect of contact time on Th⁴⁺ adsorption Adsorbent weight 0.2 g, pH of 7, 200 mg L⁻¹ Th⁴⁺ and at 25°C temperature.

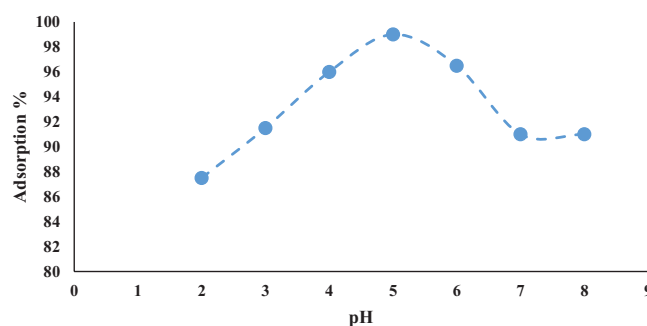


Fig. 8. Effect of pH on Th⁴⁺ adsorption. Adsorbent weight 0.2 g, contact time 70 min, 200 mg L⁻¹ Th⁴⁺ and at 25°C temperature.

adsorbed on Ch/Al-O_{NCo} increased. The maximum adsorption in the pH range 4.0–6.0 may be due to the formation of Th⁴⁺ complexes with carboxyl groups, due to its consistency constant with Th⁴⁺ [33]. Adsorption reached a maximum at a pH range 5.0–6.0. At this range, where the Th⁴⁺ removal from the solution reaches its maximum value, the governing kinds of Th⁴⁺ ions exist in solution as Th(OH)³⁺ (Fig. 9). The reduction in pH during the adsorption process, which clearly indicates the rise in the proportion of cation adsorbed, is in keeping with the occurrences of cation exchange reaction. The adsorption decreases as pH continued to increase from 6.0 to 8.0. In strong acidic solution from pH 2.0 to 4.0 hydroxonium ions H₃O⁺ compete with the positive Th⁴⁺ ions for the adsorption sites [34]. As the pH

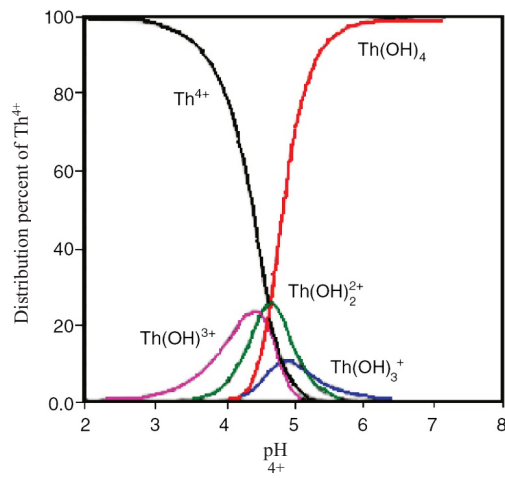


Fig. 9. Speciation of Th⁴⁺ on different pH values.

increases above 6.0, neutral tetrahydroxo form of Th⁴⁺ such as Th(OH)₄ only exist in solution. The increase in hydroxyl anion enhances the rate of formation of neutral Th(OH)₄, which decreased the rate of adsorption on Th⁴⁺ onto Ch/Al-O_{NC_o}.

3.5. Kinetic analysis

In order to investigate the controlling mechanism of adsorption process of Ch/Al-O_{NC_o} against Th⁴⁺ the pseudo-first and second-order models were used to evaluate the experimental data obtained (Figs. 10 and 11).

Adsorption rate for Ch/Al-O_{NC_o} is determined at various times under optimum adsorbent weight, contact time of 10–70 min and optimal pH at temperature 25°C. Pseudo-first-order kinetic model indicates physical adsorption process while, the pseudo-second-order kinetic model specifies that the adsorption process is chemical and exchange of electrons happens between the adsorbent and the ion being adsorbed [35–37]. Eqs. (5) and (6) show the pseudo-first and second-order kinetic model, respectively.

$$q_t = q_e (1 - e^{-k_1 t}) \tag{5}$$

$$q_t = \frac{t q_e^2}{\frac{1}{k_2} + q_e t} \tag{6}$$

where q_e ; the amount of Th⁴⁺ uptake per unit mass of adsorbent at equilibrium (mg g⁻¹), q_t ; amount of Th⁴⁺ uptake per unit mass of adsorbent at time t (mg g⁻¹), k_1 and k_2 ; reaction rate constants (mg g⁻¹ min⁻¹).

R² coefficient clearly indicates that Th⁴⁺ adsorption data on the Ch/Al-O_{NC_o} have been best described by pseudo-second-order kinetic equation, thus the rate-controlling step is chemical by complex formation/ion exchange.

3.6. Adsorption isotherms

The aim of adsorption isotherm calculation is to investigate the relationship between the amount of adsorbent and

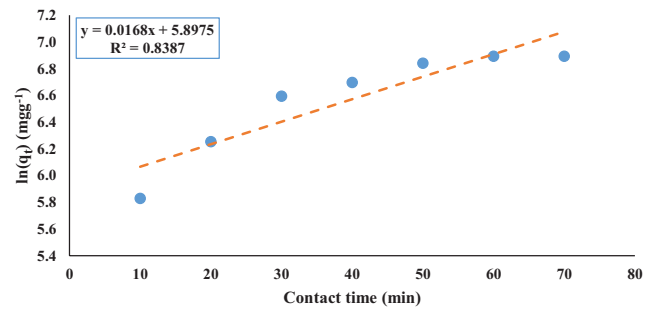


Fig. 10. Pseudo-first-order plots of Th⁴⁺ onto Ch/Al-O_{NC_o}.

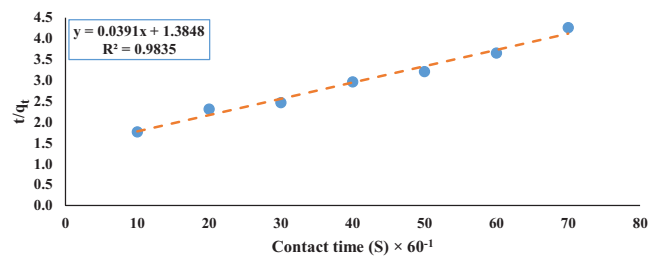


Fig. 11. Pseudo-second-order plots of Th⁴⁺ onto Ch/Al-O_{NC_o}.

Table 1
Pseudo first and second parameters

Kinetic model	Equation	q_e (mg g ⁻¹)	k_1 (min ⁻¹)	R ²
Pseudo-first-order	0.0168x+5.8975	364	0.0168	0.84
Pseudo-second-order	0.0391x+1.3848	26	0.0361	0.98

the level of adsorption during the process [38]. Langmuir, Freundlich and Dubinin–Radushkevich (D–R) isotherms were applied for analysis of adsorption equality (Figs. 12 and 13). The linearized form of the Langmuir equation which is used for monolayer adsorption on finite and similar surfaces is described by Eq. (7) [39]:

$$\frac{C_e}{q_e} = \frac{1}{K_L q_m} + \frac{C_e}{q_m} \tag{7}$$

where q_m is the maximum monolayer adsorption capacity (mg g⁻¹), K_L is the Langmuir constant related to the free energy of adsorption (L mg⁻¹), and a plot of C_e/q_e versus C_e yields a straight line with slope $1/q_m$ and intercept $1/q_m K_L$. The well-known form of the Freundlich isotherm is given by Eq. (8):

$$q_e = Kf C_e^n \tag{8}$$

which after applying logarithm for both sides, converted into Eq. (9)

$$\log(q_e) = \log(Kf) + \frac{1}{n} \log(C_e) \tag{9}$$

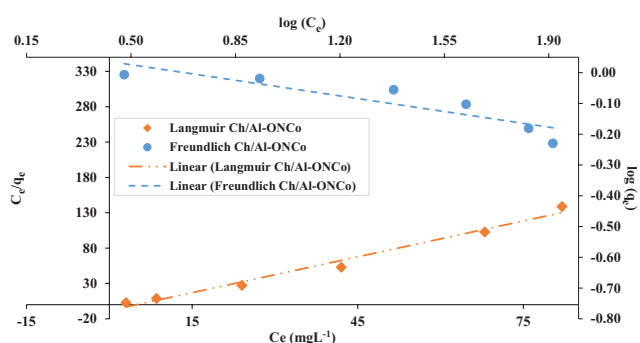


Fig. 12. Langmuir and Freundlich isotherms for adsorption of Th^{4+} on $\text{Ch/Al-O}_{\text{NCo}}$.

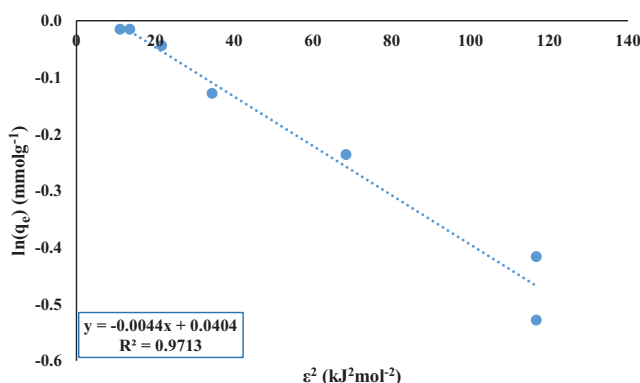


Fig. 13. Dubinin–Radushkevich (D–R) adsorption isotherm of Th^{4+} on $\text{Ch/Al-O}_{\text{NCo}}$.

where K_f and $1/n$ are the Freundlich constants related to the adsorption capacity and adsorption intensity, respectively.

Another popular isotherm model is D–R, which the non-linear and linear forms of D–R is given by Eq. (10) [40]:

$$q_e = q_{\max} e^{-K_{ad}\epsilon^2} \quad (10)$$

which the linear form can be represented by Eq. (11):

$$\ln(q_e) = \ln(q_{\max} - K_{ad}\epsilon^2) \quad (11)$$

where q_e is the amount of Th^{4+} (mmol g^{-1}) adsorbed per unit mass of $\text{Ch/Al-O}_{\text{NCo}}$, q_{\max} is the theoretical adsorption capacity (mmol g^{-1}), K_{ad} is the constant related to the adsorption energy ($\text{mol}^2 \text{kJ}^{-2}$), and ϵ is the Polanyi potential that is determined as Eq. (12):

$$\epsilon = RT \ln \left(1 + \frac{1}{C_e} \right) \quad (12)$$

where C_e is the solution concentration at equilibrium (mol L^{-1}), R is the gas constant ($8.314 \text{ J mol}^{-1} \text{ K}^{-1}$), and T is the absolute temperature of the aqueous solution (K). The amount of K_{ad} was estimated from the slope of the plot of $\ln q_e$ versus ϵ^2 and q_{\max} is prepared from the intercept. As stated, K_{ad} is related to adsorption energy, so the mean free

Table 2
Equilibrium isotherm parameters of sorption of Th^{4+} at 25°C

Isotherms		
Langmuir	Equation	$1.69x - 8.39$
	q_m (mg g^{-1})	591
	k_L (L mg^{-1})	2×10^{-4}
	R^2	0.98
Freundlich	Equation	$-0.14x + 0.09$
	K_f (mg g^{-1})	1.10
	n (gr L^{-1})	-6.91
	R^2	0.81
Dubinin–Radushkevich	Equation	$-0.0044x + 0.04$
	K_{ad} ($\text{mol}^2 \text{kJ}^{-2}$)	0.0044
	q_{\max} (mmol g^{-1})	1.04
	R^2	0.97

energy of adsorption (E) (kJ mol^{-1}), is calculated according to Eq. (13) [41]:

$$E = \frac{1}{\sqrt{2K_{ad}}} \quad (13)$$

The value of E is very effective in determining the nature of adsorption. If the value is smaller than 8 (kJ mol^{-1}), then the adsorption is physical in nature and if it is between 8 and 16 (kJ mol^{-1}), then the adsorption is chemical with an exchange of ions [42]. The value of E was found to be between 8 and 16 (kJ mol^{-1}), therefore the adsorption was chemical in nature for the $\text{Ch/Al-O}_{\text{NCo}}$, which is consistent with the results of section 3.5.

The parameters calculated from the Langmuir, Freundlich and D–R models are summarized in Table 2. The higher R^2 coefficients indicate that Langmuir model ($R^2 \geq 0.98$) fits the adsorption data better than the Freundlich and D–R model over the entire range of adsorptive concentration studied. According to Langmuir isotherm, maximum adsorption capacity was 591 mg g^{-1} at 25°C .

Table 3 presents the comparison between the maximum monolayer adsorption capacity (q_m , mg g^{-1}) of various Ch composites in the literature which indicates the high efficiency of $\text{Ch/Al-O}_{\text{NCo}}$ for Th^{4+} adsorption.

3.7. Thermodynamic studies

Thermodynamic parameters, including enthalpy change (ΔH°), Gibbs free energy change (ΔG°) and entropy change (ΔS°) can be estimated by using equilibrium constants changing with temperature. The distribution coefficient is related to the enthalpy change (ΔH°) and entropy change (ΔS°) at constant temperature ($1/T$) by the rearrangement of the Van't Hoff Eq. (14):

$$\ln(K_d) = \frac{\Delta S^\circ}{R} - \frac{\Delta H^\circ}{RT} \quad (14)$$

where K_d is the distribution coefficient (mL g^{-1}), (ΔS°) is standard entropy, (ΔH°) is standard enthalpy, T is the abso-

Table 3
Comparison between the maximum monolayer adsorption capacity (q_m , mg g⁻¹) of various adsorbents

NO.	Adsorbent	q_m (mg g ⁻¹)	Ion	References
1	Magnetic Ch composite particles	312.50	Th ⁴⁺	[30]
2	Ch/clinoptilolite	385.51	Th ⁴⁺	[2]
3	Nanoporous Magnetic Cellulose–Ch Composite Microspheres	75.82	Cu ²⁺	[41]
4	Ethylendiamine-modified magnetic Ch complex	66	UO ₂ ²⁺	[29]
5	Ch/Al-O _{NC_o}	591	Th ⁴⁺	This study

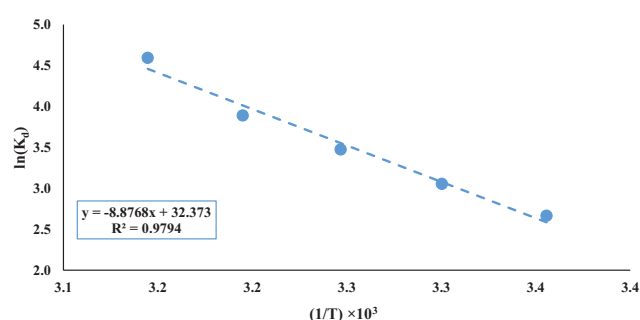


Fig. 14. Temperature dependence of the adsorption of Th⁴⁺ for Ch/Al-O_{NC_o}

lute temperature (K), R is gas constant (kJ mol⁻¹ K⁻¹). The standard free energy value is calculated from Eq. (15):

$$\Delta G^\circ = \Delta H^\circ - T\Delta S^\circ \quad (15)$$

The experiments were carried out at five temperatures (25, 30, 35, 40 and 45°C) for solution concentration of 200 mg L⁻¹ of Th⁴⁺ (Fig. 14).

The values of ΔH° and ΔS° were calculated from the slopes and intercepts of linear regression of $\ln(K_d)$ versus T^{-1} ($R^2 > 0.98$). The results in Table 4 indicate that the process is endothermic and the adsorption capacity of the Ch/Al-O_{NC_o} increases with temperature.

The positive value of ΔH° is suggestive of an endothermic nature, which favors the adsorption of Th⁴⁺ ion at higher temperature. In addition, the positive values of entropy (ΔS°) is suggestive of higher randomness of adsorption in the system and favors the stability of the adsorption. The negative values of ΔG° for these processes confirm the feasibility and spontaneous nature of adsorption process [43].

3.8. Desorption studies

The results regarding Th⁴⁺ ion desorbing percentage with various agents are shown in Table 5. The maximum Th⁴⁺ ions desorption level from the Ch/Al-O_{NC_o} (94%) was obtained by using 0.1 M HNO₃ solution. Similar findings using HNO₃ solution but in different desorption level were reported in literature [20,30]. After three cycles, the adsorption capacity of the Ch/Al-O_{NC_o} decreased from 99 to 90%, while the recovery of Th⁴⁺ ion in 0.1 M HNO₃ were reduced from 94.13% at first to 90.15%.

Table 4
Thermodynamic parameters for adsorption of Th⁴⁺ by Ch/Al-O_{NC_o}

Adsorbent	Temperature (K)	ΔG° (kJ mol ⁻¹)	ΔH° (kJ mol ⁻¹)	ΔS° (kJ K ⁻¹ mol ⁻¹)
Ch/Al-ONC _o	298	-80.0	73.621	268.671
	303	-81.3		
	308	-82.7		
	313	-84.0		
	318	-85.4		
	298	-80.0		

Table 5
Desorption results (%) in 0.1 M solution on Ch/Al-O_{NC_o} loaded with Th⁴⁺ ion

Ion	Agents			
Th ⁴⁺	NaOH	NaCl	HCl	HNO ₃
	55.17	61.22	85.67	94.13

4. Conclusion

In this study, novel Ch/Al-O_{NC_o} adsorbent was prepared and characterized and a comprehensive investigation was carried out on its adsorption capacity for the removal of Th⁴⁺ ion from aqueous solution. Th⁴⁺ ion adsorption onto the Ch/Al-O_{NC_o} was determined, namely with the adsorbent weight (0.2 g), the contact time (70 min) and pH (5). The adsorption kinetics of Th⁴⁺ on the Ch/Al-O_{NC_o} can be described by pseudo-second-order kinetic model, which indicates that adsorption involves chemical reaction. In addition, the Langmuir isotherm model excellently correlated with the experimental data. The adsorption process for Ch/Al-O_{NC_o} was spontaneous ($\Delta G^\circ < 0$) and endothermic ($\Delta H^\circ > 0$) in nature.

The results showed that the Ch/Al-O_{NC_o} has a superior adsorption capacity for Th⁴⁺ ion (591 mg g⁻¹) when compared to other adsorbents reported in the literature [2,29,30,40]. Consequently, results indicated the possibility of using the Ch/Al-O_{NC_o} for efficient removal of Th⁴⁺ ion from aqueous solutions. Finally, Th⁴⁺ ion desorption studies revealed that Th⁴⁺ ion may be recovered to the extent of over 94% when using acidic desorbing agent (0.1 M HNO₃ solution).

Acknowledgment

This research was supported by Nuclear Science and Technology Research Institute of Iran; project no. PRI-C5-93-001. The authors would like to thank the institute for providing assistance with analysis of samples carried out through this study.

List of symbols

$Ads\%$	— The adsorption percentage (%)
t	— Time (min)
q_t	— The amount of metal ion sorbed at time t ($mg\ g^{-1}$)
q_m	— The maximum monolayer adsorption capacity ($mg\ g^{-1}$)
q_e	— Amount of ion sorbed per unit mass of sorbents ($mmol\ g^{-1}$)
q_{max}	— Theoretical adsorption capacity ($mmol\ g^{-1}$)
C_o	— The initial metal ion concentration ($mg\ L^{-1}$)
C_e	— The amount of metal present in the solution at equilibrium time t ($mg\ L^{-1}$ or $mol\ L^{-1}$)
V	— The volume of metal ion concentration (L)
m	— The dry weight of sample (g)
K_d	— The ion distribution coefficient ($mL\ g^{-1}$)
k_{ad}	— Constant related to the adsorption energy ($mol^2\ kJ^{-2}$)
E	— Mean free energy of adsorption ($kJ\ mol^{-1}$)
Th^{4+}_{ads}	— The amount of adsorbed Th^{4+} ($mg\ g^{-1}$)
Th^{4+}_{des}	— The amount of desorbed Th^{4+} ($mg\ g^{-1}$)
k_1 and k_2	— Reaction rate constants ($mg\ g^{-1}\ min^{-1}$)
K_L	— The Langmuir constant related to the free energy of adsorption ($L\ mg^{-1}$)
K_f	— The Freundlich constant
n	— The Freundlich constant
ϵ	— Polanyi potential
ΔH°	— Enthalpy change ($kJ\ mol^{-1}$)
ΔG°	— Gibbs free energy change ($kJ\ mol^{-1}$)
ΔS°	— Entropy change ($kJ\ K^{-1}\ mol^{-1}$)
T	— Temperature ($^\circ C$ or K)
R	— Gas constant ($kJ\ mol^{-1}\ K^{-1}$)

References

- [1] S. Balasubramaniana, Chitosan-Based Polymer Nanocomposites for Heavy Metal Removal, Nanocomposites in Wastewater Treatment Pan Stanford Publishing, Pte, 2014.
- [2] D. Humelnicu, M.V. Dinu, E.S. Drăgan, Adsorption characteristics of UO_2^{2+} and Th^{4+} ions from simulated radioactive solutions onto chitosan/clinoptilolite sorbents, *J. Hazard. Mater.*, 185 (2011) 447–455.
- [3] V. Jain, R. Pandya, S. Pillai, P. Shrivastav, Simultaneous preconcentration of uranium (VI) and thorium (IV) from aqueous solutions using a chelating calix [4] arene anchored chloromethylated polystyrene solid phase, *Talanta*, 70 (2006) 257–266.
- [4] A. Nilchi, T.S. Dehaghan, S.R. Garmarodi, Kinetics, isotherm and thermodynamics for uranium and thorium ions adsorption from aqueous solutions by crystalline tin oxide nanoparticles, *Desalination*, 321 (2013) 67–71.
- [5] T.P. Rao, P. Metilda, J.M. Gladis, Preconcentration techniques for uranium (VI) and thorium (IV) prior to analytical determination—an overview, *Talanta*, 68 (2006) 1047–1064.
- [6] P. Vijayan, I. Dulera, P. Krishnani, K. Vaze, S. Basu, R. Sinha, Overview of the thorium programme in India, *Thorium Energy for the World*, Springer 2016, pp. 59–69.
- [7] T. Prasada Rao, P. Metilda, J. Mary Gladis, Preconcentration techniques for uranium (VI) and thorium (IV) prior to analytical determination— an overview, *Talanta*, 68 (2006) 1047–1064.
- [8] V. Höllriegl, M. Greiter, A. Giussani, U. Gerstmann, B. Michalke, P. Roth, U. Oeh, Observation of changes in urinary excretion of thorium in humans following ingestion of a therapeutic soil, *J. Environ. Radioactiv.*, (2007) 149–160.
- [9] F.A. Aydin, M. Soylak, A novel multi-element coprecipitation technique for separation and enrichment of metal ions in environmental samples, *Talanta*, 73 (2007) 134–141.
- [10] W.H. Brattain, J.A. Becker, Thermionic and adsorption characteristics of thorium on tungsten, *Phys. Rev.*, 43 (1933) 428.
- [11] A. Jyothi, G. Rao, Solvent extraction behaviour of lanthanum (III), cerium (III), europium (III), thorium (IV) and uranium (VI) with 3-phenyl-4-benzoyl-5-isoxazolone, *Talanta*, 37 (1990) 431–433.
- [12] K.A. Kraus, G.E. Moore, F. Nelson, Anion-exchange Studies. XXI. Th (IV) and U (IV) in hydrochloric acid. separation of thorium, protactinium and uranium 1, 2, *J. Amer. Chem. Soc.*, 78 (1956) 2692–2695.
- [13] Z. Shiri-Yekta, M.R. Yaftian, A. Nilchi, Silica nanoparticles modified with a Schiff base ligand: an efficient adsorbent for Th (IV), U (VI) and Eu (III) ions, *Korean J. Chem. Eng.*, 30 (2013) 1644–1651.
- [14] C.W. Sill, C. Willis, Precipitation of submicrogram quantities of thorium by barium sulfate and application to the fluorometric determination of thorium in mineralogical and biological samples, *Anal. Chem.*, 36 (1964) 622–630.
- [15] M. Tsezos, B. Volesky, Biosorption of uranium and thorium, *Biotech. Bioeng.*, 23 (1981) 583–604.
- [16] D. Zhang, S. Wei, C. Kaila, X. Su, J. Wu, A.B. Karki, D.P. Young, Z. Guo, Carbon-stabilized iron nanoparticles for environmental remediation, *Nanosca*, 2 (2010) 917–919.
- [17] S. Pollard, G. Fowler, C. Sollars, R. Perry, Low-cost adsorbents for waste and wastewater treatment: a review, *Sci. Tot. Environ.*, 116 (1992) 31–52.
- [18] A. Rahmati, A. Ghaemi, M. Samadfam, Kinetic and thermodynamic studies of uranium (VI) adsorption using Amberlite IRA-910 resin, *Annal. Nucl. Ener.*, 39 (2012) 42–48.
- [19] N.Q. Hien, D. Van Phu, N.N. Duy, H.T. Huy, Radiation grafting of acrylic acid onto partially deacetylated chitin for metal ion adsorbent, *Nuclear Instrum. Methods Phys. Res. Sec. B: Beam Interact. Mat. Atom.*, 236 (2005) 606–610.
- [20] T.S. Anirudhan, S. Rijith, A.R. Tharun, Adsorptive removal of thorium (IV) from aqueous solutions using poly (methacrylic acid)-grafted chitosan/bentonite composite matrix: process design and equilibrium studies, *Colloid. Surf. A: Physicochem. Eng. Asp.*, 368 (2010) 13–22.
- [21] H. Yi, L.-Q. Wu, W.E. Bentley, R. Ghodssi, G.W. Rubloff, J.N. Culver, G.F. Payne, Biofabrication with chitosan, *Biomacromol.*, 6 (2005) 2881–2894.
- [22] D. Mohan, C.U. Pittman, Activated carbons and low cost adsorbents for remediation of tri- and hexavalent chromium from water, *J. Hazard. Mater.*, 137 (2006) 762–811.
- [23] M. Saifuddin, P. Kumaran, Removal of heavy metal from industrial wastewater using chitosan coated oil palm shell charcoal, *Elect. J. Biotechnol.*, 8 (2005) 43–53.
- [24] C. Gerente, V. Lee, P.L. Cloirec, G. McKay, Application of chitosan for the removal of metals from wastewaters by adsorption—mechanisms and models review, *Critic. Rev. Environ. Sci. Technol.*, 37 (2007) 41–127.
- [25] J. Jordan, K.I. Jacob, R. Tannenbaum, M.A. Sharaf, I. Jasiuk, Experimental trends in polymer nanocomposites—a review, *Mater. Sci. Eng. A*, 393 (2005) 1–11.
- [26] W.W. Ngah, L. Teong, M. Hanafiah, Adsorption of dyes and heavy metal ions by chitosan composites: A review, *Carbohydr. Polym.*, 83 (2011) 1446–1456.
- [27] R. Akkaya, U. Ulusoy, Adsorptive features of chitosan entrapped in polyacrylamide hydrogel for Pb^{2+} , UO_2^{2+} , and Th^{4+} , *J. Hazard. Mater.*, 151 (2008) 380–388.
- [28] R.A. Muzzarelli, Potential of chitin/chitosan-bearing materials for uranium recovery: An interdisciplinary review, *Carbohydr. Polym.*, 84 (2011) 54–63.

- [29] J.-s. Wang, R.-t. Peng, J.-h. Yang, Y.-c. Liu, X.-j. Hu, Preparation of ethylenediamine-modified magnetic chitosan complex for adsorption of uranyl ions, *Carbohydr. Polym.*, 84 (2011) 1169–1175.
- [30] D. Hritcu, D. Humelnicu, G. Dodi, M.I. Popa, Magnetic chitosan composite particles: evaluation of thorium and uranyl ion adsorption from aqueous solutions, *Carbohydr. Polym.*, 87 (2012) 1185–1191.
- [31] K. Ogawa, S. Hirano, T. Miyanishi, T. Yui, T. Watanabe, A new polymorph of chitosan, *Macromolec.*, 17 (1984) 973–975.
- [32] J. Acharya, J. Sahu, C. Mohanty, B. Meikap, Removal of lead (II) from wastewater by activated carbon developed from Tamarind wood by zinc chloride activation, *Chem. Eng. J.*, 149 (2009) 249–262.
- [33] D. Langmuir, J.S. Herman, The mobility of thorium in natural waters at low temperatures, *Geochim. Cosmochim. Acta.*, 44 (1980) 1753–1766.
- [34] S. Savvin, Analytical use of arsenazo III: determination of thorium, zirconium, uranium and rare earth elements, *Talanta*, 8 (1961) 673–685.
- [35] J.F. Corbett, Pseudo first-order kinetics, *J. Chem. Educ.*, 49 (1972) 663.
- [36] F.-C. Wu, R.-L. Tseng, S.-C. Huang, R.-S. Juang, Characteristics of pseudo-second-order kinetic model for liquid-phase adsorption: A mini-review, *Chem. Eng. J.*, 151 (2009) 1–9.
- [37] H. Yuh-Shan, Citation review of Lagergren kinetic rate equation on adsorption reactions, *Scientomet.*, 59 (2004) 171–177.
- [38] B. Hameed, D. Mahmoud, A. Ahmad, Equilibrium modeling and kinetic studies on the adsorption of basic dye by a low-cost adsorbent: Coconut (*Cocos nucifera*) bunch waste, *J. Hazard. Mater.*, 158 (2008) 65–72.
- [39] Y. Wu, S.-Y. Kim, D. Tozawa, T. Ito, T. Tada, K. Hitomi, E. Kuraoka, H. Yamazaki, K. Ishii, Equilibrium and kinetic studies of selective adsorption and separation for strontium using DtBuCH18C6 loaded resin, *J. Nucl. Sci. Technol.*, 49 (2012) 320–327.
- [40] E. Metwally, T. El-Zakla, R. Ayoub, Thermodynamics study for the sorption of ^{134}Cs and ^{60}Co radionuclides from aqueous solutions, *J. Nucl. Radiochem. Sci.*, 9 (2008) 1–6.
- [41] M. Ghasemi, M. Naushad, N. Ghasemi, Y. Khosravi-Fard, Adsorption of Pb (II) from aqueous solution using new adsorbents prepared from agricultural waste: adsorption isotherm and kinetic studies, *J. Ind. Eng. Chem.*, 20 (2014) 2193–2199.
- [42] A. Dada, A. Olalekan, A. Olatunya, O. Dada, Langmuir, Freundlich, Temkin and Dubinin–Radushkevich isotherms studies of equilibrium sorption of Zn^{2+} onto phosphoric acid modified rice husk, *IOSR, J. Appl. Chem.*, 3 (2012) 38–45.
- [43] P. Ilaiyaraja, A.K.S. Deb, K. Sivasubramanian, D. Ponraju, B. Venkatraman, Adsorption of uranium from aqueous solution by PAMAM dendron functionalized styrene divinylbenzene, *J. Hazard. Mater.*, 250 (2013) 155–166.